Volume 1 | Number 1 | Jan 2013 | Pages 1–100

Nanoscale

www.rsc.org/nanoscale

ROYAL SOCIETY
OF CHEMISTRY

This is an *Accepted Manuscript*, which has been through the Royal Society of Chemistry peer review process and has been accepted for publication.

Accepted Manuscripts are published online shortly after acceptance, before technical editing, formatting and proof reading. Using this free service, authors can make their results available to the community, in citable form, before we publish the edited article. We will replace this *Accepted Manuscript* with the edited and formatted *Advance Article* as soon as it is available.

You can find more information about *Accepted Manuscripts* in the **Information for Authors**.

ROYAL SOCIETY
OF CHEMISTRY

www.rsc.org/nanoscale

Nanoscale

ARTICLE

Dynamically configurable hybridization of plasmon modes in nanoring dimer arrays

Lei Zhang,[a†] Zhaogang Dong,[b] Ying Min Wang,[b] Yan Jun Liu,[b] Shuang Zhang,[c] Joel Kwang Wei Yang[b,d] and Cheng-Wei Qiu[a,e†]

We present a novel strategy capable of dynamically configuring the plasmon-induced transparency (PIT) effect with polarization-dependent controllability based on a nanoring dimer array. The controllable coupling strength between the superradiant and subradiant modes is owing to the polarization-dependent field distributions. It is shown that the dynamically controlled PIT is realized with a modulation depth as high as 95%, and a linear dependence of the coupling strength on polarization angle is deduced using a coupled-oscillator model. We believe that our results will inspire further exciting achievements that utilize various polarization states of the electromagnetic wave and pave a way towards applications using PIT with dynamic controllability, such as slow light, optical nonlinearities and chemical/bio-sensing.

Introduction

Fano resonance, resulting from hybridizing a broadband superradiant and a narrowband subradiant modes,[1, 2] has drawn great interest due to its versatility in near-field control[3, 4] and far-field response.[5] A myriad of applications have been explored, such as sensing,[6, 7] plasmonic trapping,[8] and nonlinear optical effect enhancement.[9, 10] As a special case, the plasmon-induced transparency (PIT) resulting from coupling of slightly detuned two modes has been demonstrated by stacking a metallic nanorod, providing a broadband mode, on a pair of metallic nanowire, acting as a narrowband mode, either horizontally or vertically.[11, 12] However, due to the anisotropic electromagnetic response of the building blocks, previous demonstrations lack of dynamical controllability because the coupling between two resonances is dependent on their relative separation, which is fixed for a given design. It is thus challenging to achieve dynamically controlled transparency with the existing designs.

Here, we would like to emphasize that the essence of coupling lies on the spatial overlap of the field distributions,

rather than merely the physical separation of structures. Usually, the overlap area is enlarged by moving two structures towards each other. If such overlap area can be controlled with an alternative approach, the coupling strength can be controlled equally. As one potential candidate, polarization is capable of rotating the corresponding field nodes of the respective modes so as to tune their coupling efficiency. However, there has yet been a thorough investigation on the dynamic control of PIT effect by tuning polarization, although polarization has been applied to dynamically engineer resonant modes for different applications, such as plasmonic trapping and rotating.[13] Especially, more polarization states have been realized, such as radially and azimuthally polarized states. Therefore, it is of realistic significance to study the influence of polarization states on the resonant response of a system.

In this work, we propose a novel strategy to achieve dynamically controlled hybridization based on a dissimilar nanoring dimer.[14-16] As a demonstration, a polarization-controlled PIT effect is investigated both numerically and experimentally. By rotating the polarization of incident light, the entire system can convert from opaque to transparent and *vice versa*, with a modulation depth as high as 95%. Furthermore, it is found that coupling strength is approximately linearly proportional to the polarization angle, which opens up a novel mechanism in controlling mode interaction. Our proposed scheme expands the current understanding on mode coupling, which will inspire promising applications of using nanoplasmonic devices with a polarization-enabled controllability.

a. Department of Electrical and Computer Engineering, National University of Singapore, Singapore 117583, Singapore.
b. Institute of Materials Research and Engineering, Agency for Science, Technology and Research (A*STAR), Singapore 117602, Singapore.
c. School of Physics and Astronomy, University of Birmingham, Birmingham B15 2TT, UK.
d. Singapore University of Technology and Design, Singapore 138682, Singapore.
e. SZU-NUS Collaborative Innovation Center for Optoelectronic Science and Technology, Shenzhen University, Guangdong 518060, China.
† Corresponding email: elezlei@nus.edu.sg or eleqc@nus.edu.sg
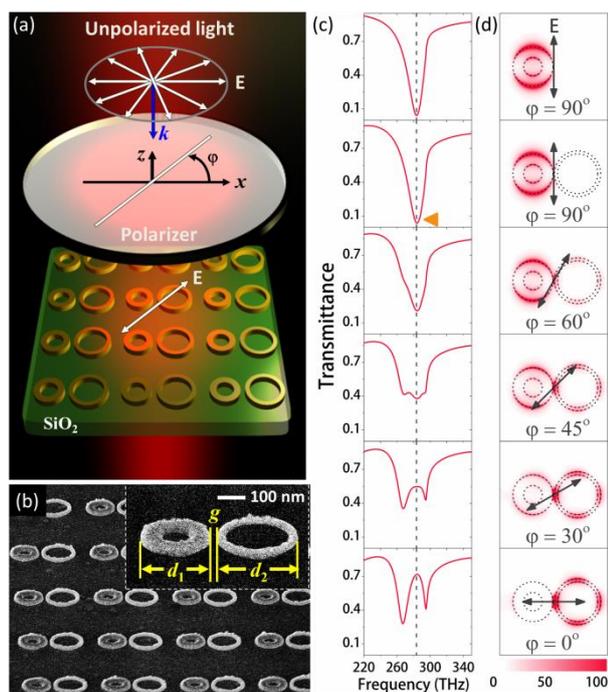
Fig. 1 (a) Schematic of the proposed structure. (b) Angled-view scanning electron micrograph (SEM) of the sample fabricated by electron beam lithography (EBL) showing an array of nanoring dimers. (c) Simulated transmittance spectra under illumination with different polarization angles. Diameters d_1 = 260 nm and d_2 = 300 nm. (d) Electric field intensity distribution at a plane 2 nm above structures at the frequency 285.4 THz as indicated by the dashed line in column (c). For all the simulations: the height of nanoring is 40 nm; the gap g is 10 nm; the periodicity is 700 nm; the wall thicknesses of left and right nanorings are 70 nm and 20 nm, respectively.

Results and discussion

The unit cell of the proposed design consists of two dissimilar nanorings separated by a small gap, as shown in Fig. 1a. A representative SEM image of the fabricated sample is taken at a tilted angle of 45°, as shown in Fig. 1b. The dimensions of the two nanorings are chosen carefully so that the resonances of the superradiant dipolar mode of the left nanoring and the subradiant quadrupolar mode of the right nanoring are closely aligned in frequency. As a reference, when there is only one left nanoring, a transmission dip in the first row in Fig. 1c, arises from the strong absorption caused by exciting the superradiant mode, which is shown by the dipolar field distribution in the first row of Fig. 1d.

When a second nanoring supporting the superradiant mode is introduced at a separation of 10 nm, the change in transmittance is negligible when the polarization angle is perpendicular to the x-axis, i.e. $\varphi = 90^{\circ}$, as shown in the second row of Fig. 1c. In this case, the quadrupolar mode can be excited neither by far field nor by near field. The former can be attributed to lack of a net dipole moment under normal incidence. On the other hand, the latter is because the antinodes of the dipolar field are far away from the ones of the

quadrupolar mode, as shown in the second row of Fig. 1d. As a result, there exists a negligible coupling between them and no perceivable difference in field distributions was found. Through rotating the polarization in a clockwise manner, one antinode of the dipolar field gradually approaches the quadrupolar field antinodes. Their coupling strength increases resulting from their energy exchange. With such exchange, partially destructive interference between two pathways exciting superradiant mode weakens the coupling of incident energy into system and leads to an increase in transmission, while the electric field starts to distribute around the right nanoring. When the electric field is polarized along the x-axis, i.e. $\varphi = 0^{\circ}$, the field antinodes are aligned to achieve the maximum coupling strength. This effect, in turn, maximizes the destructive interference and the entire system becomes transparent with a transmittance of 0.72, which is much higher than the transmittance of 0.036 supported when $\varphi = 90^{\circ}$. Simultaneously, the electric field is mainly confined around the right nanoring rendering a quadrupolar distribution, while the dipolar field distribution of the left nanoring disappears, which leads to an inefficient absorption of the incident optical field and thus a high transmittance. The resultant modulation depth, defined as $| (T_{on} - T_{off}) / T_{on}| \times 100\%$, reaches as high 95%, where T_{on} and T_{off} represent the transmittance with the maximized PIT and without PIT effect, respectively. It should be pointed that the field distributions of dipolar and quadrupolar modes of nanorings possess C2 and C4 symmetry respectively. The field distribution of quadrupolar mode keeps the same under both polarization $\varphi = 90^{\circ}$ and $\varphi = 0^{\circ}$. All the spectrum changes caused by polarization rotation arise from the rotation of dipolar mode, which is different from coupling between two dipolar modes.

Coupling strength between two superradiant modes using two identical nanoring dimers is able to be controlled by varying their separation distance as discussed in the literature.[17, 18] However, to the best of our knowledge, the specific mode coupling controlled by polarization has yet to be discussed in the context of the interactions between the superradiant and the subradiant modes. Here, a small nanoring is chosen to support a superradiant mode with a resonance frequency of 285.4 THz. The full-width at half maximum (FWHM) is 26.1 THz as obtained by fitting the transmittance spectrum with a Lorentzian function. The transmission dip will flip over as a peak when a larger nanoring supporting subradiant mode is placed on its right side. The difference in dip and peak positions could be attributed to the slight mismatch between the resonance frequencies of two modes, which coincide with each other as d_2 reaches 300 nm shown in Fig. 2a.

The strong coupling between the superradiant and subradiant modes can be understood with a typical three-level system shown in Fig. 2b.[12, 19, 20] $|0\rangle$ represents the ground state; $|1\rangle$ and $|2\rangle$ are the excited states, which represent the superradiant mode and subradiant mode, respectively. The field distributions of E_z component shown in Fig. 2b&c are plotted at a plane 2 nm above the structure surface, indicating
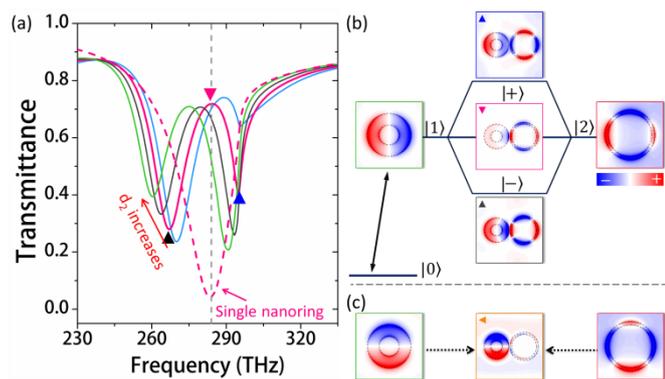
Fig. 2 (a) Transmittance evolves as the diameter d_2 increases from 290 nm to 320 nm with a step 10 nm, where diameter d_1 = 260 nm and the wall thicknesses of left and right nanorings are 70 nm and 20 nm, respectively; polarization angle φ = 0°. The transmittance of single nanoring with diameter d = 260 nm is plotted as a reference indicated by the dashed line. (b) Field distribution of E_z component under excitation with polarization angle of φ = 0°, indicating a strong coupling. (c) Field distribution of E_z component under the excitation with polarization angle of φ = 90°, indicating a weak coupling. Field distributions are calculated under normal illumination except for quadrupolar mode, simulated with an incident angle of 30°.

the corresponding surface charge distributions.[21] Under far-field excitation, $|0\rangle \rightarrow |1\rangle$ is a dipole-allowed transition, while $|0\rangle \rightarrow |2\rangle$ is a dipole-forbidden one under normal incidence. However, it becomes allowable under inclined illumination due to the retardation effect, indicating by a distorted quadrupolar field distribution shown in Fig. 2b. Besides far-field excitation, near-field coupling is another way to excite the subradiant mode. When the superradiant mode is in a close proximity to the subradiant one, the strong near-field of $|1\rangle$ could excite $|2\rangle$ and *vice versa*. As a result, there exist two pathways to excite the superradiant mode, *i.e.* $|0\rangle \rightarrow |1\rangle$ and $|0\rangle \rightarrow |1\rangle \rightarrow |2\rangle \rightarrow |1\rangle$. When they interfere destructively, the dipolar field almost diminishes, which is obviously exhibited by the field distribution as labelled by a pink-downward triangle in Fig. 2b. Therefore, both reflection and absorption could be extremely suppressed, and the entire system will become transparent to give rise to the PIT effect.

Concomitantly, two sharp transmission dips originate from the coupling between $|1\rangle$ and $|2\rangle$. From the perspective of mode hybridization, the original energy state splits into two hybridized modes with one at high frequency $|+\rangle$ and the other at low frequency $|-\rangle$. As a result, a band gap opens up at the original frequency, which results in a transparent window due to an inefficient light absorption. In this sense, the PIT effect could be considered as a byproduct of mode hybridization. It is remarkable that the FWHM of the lower frequency resonance is only 16.6 THz, which is even smaller than the Drude damping limit of Rayleigh nanoparticles (18 THz).[22] Generally, for a given system, the decay rate of a mode is determined by the ratio of the volume of the conductor into

which the fields penetrate because of the finite conductivity over the volume occupied by the fields. It indicates that the decay properties of a mode could be tuned by distorting the field distribution,[23] which has been verified in ref. 12. In our case, the reduction in decay rate arises from the effective suppression of the radiative dissipation as well as the intrinsic absorption. The latter is mainly caused by a significant amount of electric field being spreading out of metallic parts, during energy circulating between two nanorings. The energy ratio absorbed by the metallic part is only 41% at 267.4 THz, which is also smaller than the counterpart of Rayleigh particles, *i.e.* 57%.[22] Furthermore, it is found that there is no energy flow between neighbouring unit cell as shown in supporting information (SI). Therefore, the narrow peaks observed in our proposed system must result from the energy decay within one unit cell. On the other hand, the linewidth of the higher frequency mode is only 10.4 THz. Both the localized coupling between the superradiant-subradiant modes and diffraction effect contribute to such a drastically narrow linewidth.[6, 24, 25] It thus implies that this compound system provides an efficient approach to decelerate the dissipation process of plasmon, which has a great potential for applications such as sensing, light emission, and solar cells.

From a system perspective, two nanorings can be deemed as a whole. As a result, the final mode of the system should result from the interplay of two fundamental modes on each nanoring. The first and second modes, containing both obvious dipolar and quadruplar field distributions, can be excited at polarization angle φ = 0°, as shown in Fig. 2b. They can differentiate from the π-phase difference between the fields at both sides of the gap. The third mode of the system is identified with field distribution shown in Fig. 2c at polarization angle of φ = 90°, where the dipolar field is clearly rendered but the quadrupolar field is very weak. In this connection, there are three modes overall supported at the frequency range of interest. However, it is worth emphasizing that these three modes originate from strong or weak coupling of dipolar and quadrupolar modes. In other words, the latter two modes are the essential cause of the phenomenon observed in this system. Therefore, to quantitatively explore coupling in a dissimilar nanoring dimer system, only two modes, *i.e.* the dipolar mode and quadrupolar mode, are involved in the coupled Lorentz oscillator model.[11, 12, 26] The amplitude of superradiant dipolar mode A_1 can be obtained as

$$|A_1| = \left| \frac{\eta(-\omega + \omega_2 - i\gamma_2/2)}{(-\omega + \omega_1 - i\gamma_1/2)(-\omega + \omega_2 - i\gamma_2/2) - \kappa^2} E_0 + bg \right| \quad (1)$$

which can interact with incoming light directly with a geometric factor η. The other oscillator denoting the subradiant mode can be excited through near-field coupling with a coupling strength of κ. γ_j is the damping rate. E_0 is the amplitude of incident field. Since the incident energy is not perfectly coupled into the superradiant dipole mode, a constant field component bg should be taken into account as a background.[8, 27, 28]

ARTICLE   **Nanoscale**
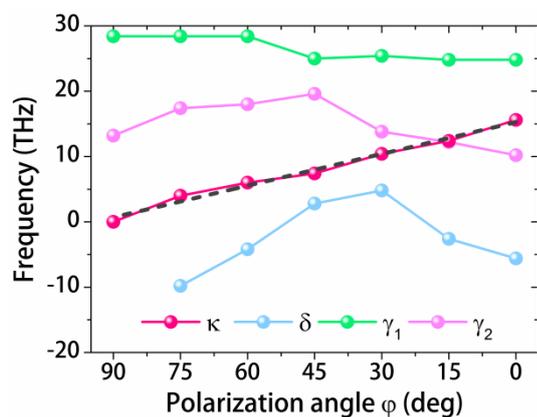
Fig. 3 Retrieved coupling and damping parameters against polarization angles. Black dashed line shows the linear fitting of coupling strength against polarization angle φ.

To unveil the interaction between two fundamental modes, the coupling and damping parameters can be obtained by fitting the magnitudes of electric field with eqn (1). The retrieved parameters are plotted in Fig. 3. When the polarization angle φ is 90°, the fitted damping rate γ_1 of superradiant mode is 28.4 THz, which matches well with the value of single dipolar mode by fitting with a Lorentzian function; the estimated damping rate γ_2 of subradiant quadrupole mode is simply set to be 14.0 THz, which is obtained from inclined illumination of single quadrupolar mode. κ is set as 0 due to a negligible coupling. Significantly, the coupling strength κ is approximately linearly proportional to the polarization angle and it increases as polarization angle decreases owing to a better alignment of field antinodes between two modes, see a detailed discussion in SI. Such a novel scheme in controlling mode coupling has a great potential in plasmonic devices. Notably, there are also slight changes in fitted decay rates, which may be beyond the general consideration. Usually, as one of the intrinsic properties of a given mode, the decay rate is known as a constant. However, this statement may not be appropriate for a more general case when field distributions have distortions.[23] Due to the strong coupling, the field profiles around each nanoring deviate from the corresponding eigenmodes. Therefore, the observed decay rate may also include the contributions from other eigenmodes, which leads to a change in the decay rate. Accordingly, it is reasonable that the decay rate varies in our work, which results from the distorted fields by gradually rotating the polarization clockwise, as shown in Fig. 1d. Polarization-dependent excitation could thus provide a feasible approach to engineer the decay properties of plasmonic resonances. It should be noted that the coupled oscillator model well explains the main features of the proposed system. However, the real system is much more complicated. For instance, the coupling strength could be a complex value instead of real quantity when an additional phase factor is taken into account.[29]
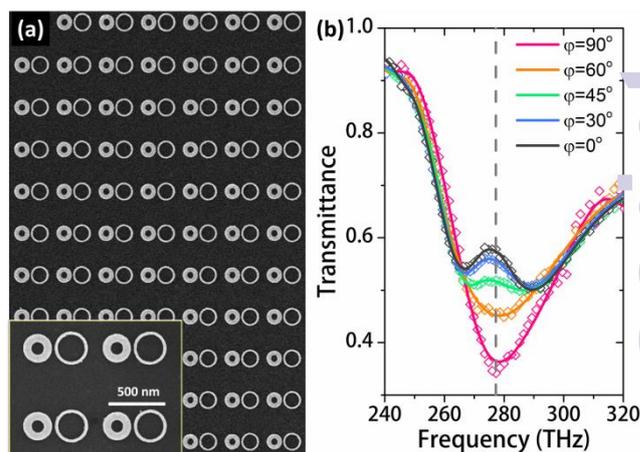
Fig. 4 (a) Top view of SEM image of the fabricated sample. Inset shows the close-up SEM image. d_1 = 254 nm, d_2 = 300 nm, g = 20 nm, periodicity = 700 nm, and the wall thicknesses of two nanorings are 7? nm and 29 nm. (b) Transmittance spectra measured under illumina with different polarizations.

The proposed polarization-dependent PIT device experimentally verified *via* the sample fabricated by EBL. A the polarization of incident light rotates from 90° to 0°, the transmittance increases from 0.34 to 0.58 at frequency 275. THz, as shown in Fig. 4b, reaching a maximum as the electr field oscillates along the center-to-center axis of two nanorings. The modulation depth achieved experimentally thus 41%, which is smaller than the 93.9% obtained in simulation with g = 20 nm. The difference between th theoretically calculation and the experimental measurement can be largely attributed to grain boundaries, large damping caused by the adhesion layer, and deviations from a perfect normal excitation. Nonetheless, the trends in our experiment findings support the validity of our theoretical predictions, clearly demonstrating the feasibility of polarization-ba dynamic control of the PIT effect exhibited by the propose nanoring dimer structure. Although the polarization-dependent transparency has been investigated before, the working mechanisms, relying either on the control of phas difference of two bright modes or on the turning on/off th dark mode, are quite different from ours.[30, 31]

Conclusions

In summary, a novel strategy of realizing dynamical controllable hybridization of plasmon modes was proposed based on dissimilar nanoring dimer arrays. As a demonstration the polarization-controlled PIT effect was investigated bot numerically and experimentally. Through aligning the fiel antinodes of superradiant mode with the subradiant one b rotating polarization, the entire structure undergoes transition from opaque to transparent. The modulation dept achieved was calculated to be as high as 95%. The couplin strength between two modes is linearly proportional to th polarization angle as shown by using a coupled oscillato

model. Our proposed structure demonstrated a promising approach in controlling both near-field coupling and far-field response with dynamic tunability by simply controlling the incident polarization. Lastly, we believe that the dynamical manipulation strategy will inspire other exciting achievements by utilizing polarization states of electromagnetic wave.

Acknowledgements

Notes and references

1. A. E. Miroshnichenko, S. Flach and Y. S. Kivshar, *Rev. Mod. Phys.* 2010, **82**, 2257-2298.

2. B. Luk'yanchuk, N. I. Zheludev, S. A. Maier, N. J. Halas, P. Nordlander, H. Giessen and C. T. Chong, *Nat. Mater.*, 2010, **9**, 707-715.

3. J. Ye, F. Wen, H. Sobhani, J. B. Lassiter, P. V. Dorpe, P. Nordlander and N. J. Halas, *Nano Lett.*, 2012, **12**, 1660-1667.

4. S. Campione, C. Guclu, R. Ragan and F. Capolino, *ACS Photon.*, 2014, **1**, 254-260.

5. B. Gallinet and O. J. F. Martin, *ACS Nano*, 2011, **5**, 8999-9008.

6. L. Zhang, C. Y. Chan, J. Li and H. C. Ong, *Opt. Express*, 2012, **20**, 12610-12621.

7. Y. Zhan, D. Y. Lei, X. Li and S. A. Maier, *Nanoscale*, 2014, **6**, 4705-4715.

8. Z. Li, S. Zhang, L. Tong, P. Wang, B. Dong and H. Xu, *ACS Nano*, 2013, **8**, 701-708.

9. G. F. Walsh and L. Dal Negro, *Nano Lett.* 2013, **13**, 3111-3117.

10. Y. Zhang, F. Wen, Y.-R. Zhen, P. Nordlander and N. J. Halas, *Proc. Natl. Aca. Sci. U.S.A.*, 2013, **110**, 9215-9219.

11. S. Zhang, D. A. Genov, Y. Wang, M. Liu and X. Zhang, *Phys. Rev. Lett.*, 2008, **101**, 047401.

12. N. Liu, L. Langguth, T. Weiss, J. Kastel, M. Fleischhauer, T. Pfau and H. Giessen, *Nat. Mater.*, 2009, **8**, 758-762.

13. K. Wang, E. Schonbrun, P. Steinvurzel and K. B. Crozier, *Nat. Commun.*, 2011, **2**, 469.

14. J. Aizpurua, P. Hanarp, D. S. Sutherland, M. Käll, G. W. Bryant and F. J. García de Abajo, *Phys. Rev. Lett.*, 2003, **90**, 057401.

15. Y. Cai, Y. Li, P. Nordlander and P. S. Cremer, *Nano Lett.*, 2012, **12**, 4881-4888.

16. H. Liu, E. S. P. Leong, Z. Wang, G. Si, L. Zheng, Y. J. Liu and C. Soci, *Adv. Opt. Mater.*, 2013, **1**, 978-983.

17. R. Near, C. Tabor, J. Duan, R. Pachter and M. El-Sayed, *Nano Lett.*, 2012, **12**, 2158-2164.

18. C.-Y. Tsai, J.-W. Lin, C.-Y. Wu, P.-T. Lin, T.-W. Lu and P.-T. Lee, *Nano Lett.*, 2012, **12**, 1648-1654.

19. M. Fleischhauer, A. Imamoglu and J. P. Marangos, *Rev. Mod. Phys.*, 2005, **77**, 633-673.

20. T. J. Davis, D. E. Gómez and K. C. Vernon, *Nano Lett.*, 20, **10**, 2618-2625.

21. A. Lovera, B. Gallinet, P. Nordlander and O. J. F. Martin, *ACS Nano*, 2013, **7**, 4527-4536.

22. F. Wang and Y. R. Shen, *Phys. Rev. Lett.*, 2006, **97**, 206806.

23. J. D. Jackson, *Classical Electrodynamics*, John Wiley & Sons, New York, 1975.

24. V. G. Kravets, F. Schedin and A. N. Grigorenko, *Phys. Rev. Lett.*, 2008, **101**, 087403.

25. A. A. Yanik, A. E. Cetin, M. Huang, A. Artar, S. H. Mousavi, A. Khanikaev, J. H. Connor, G. Shvets and H. Altug, *Proc. Natl. Aca. Sci. U.S.A.* 2011, **108**, 11784-11789.

26. S. Zhang, Z. Ye, Y. Wang, Y. Park, G. Bartal, M. Mrejen, X. Yi and X. Zhang, *Phys. Rev. Lett.*, 2012, **109**, 193902.

27. C. Ropers, D. J. Park, G. Stibenz, G. Steinmeyer, J. Kim, D. S Kim and C. Lienau, *Phys. Rev. Lett.*, 2005, **94**, 113901.

28. A. Christ, Y. Ekinci, H. H. Solak, N. A. Gippius, S. G. Tikhod and O. J. F. Martin, *Phys. Rev. B*, 2007, **76**, 201405.

29. R. Taubert, M. Hentschel, J. Kästel and H. Giessen, *Nano L* 2012, **12**, 1367-1371.

30. J. Chen, P. Wang, C. Chen, Y. Lu, H. Ming and Q. Zhan, *Opt. Express*, 2011, **19**, 5970-5978.

31. W.-S. Chang, J. B. Lassiter, P. Swanglap, H. Sobhani, S Khatua, P. Nordlander, N. J. Halas and S. Link, *Nano Lett.*, 2012, **12**, 4977-4982.